Maximum deflection of a blast loaded circular flat plate
by George Thomas Nolan

A thesis submitted to the Graduate Faculty in partial fulfillment of the requirements for the degree of
MASTER OF SCIENCE in Mechanical Engineering
Montana State University

Abstract:
The purpose of this paper is to present an analytical method for calculating the maximum deflection of a simply supported circular flat plate which is subjected to a blast loading. The method is based on the Modified Galerkin Method, and uses a non-linear stress-strain relationship together with non-linear geometry. Equations of equilibrium are reduced to an ordinary differential equation which, when solved, yields an approximation of the maximum plate deflection.

Calculated maximum deflections are compared to experimental test results of permanently deformed plates.

The calculated deflections are approximately 72% of the magnitude of the test results.

In presenting this thesis in partial fulfillment of the requirements for an advanced degree at Montana State University, I agree that the Library shall make it freely available for inspection. I further agree that permission for extensive copying of this thesis for scholarly purposes may be granted by my major professor, or, in his absence, by the Director of Libraries. It is understood that any copying or publication of this thesis for financial gain shall not be allowed without my written permission.

Signature 

Date July 24, 1969

MAXIMUM DEFLECTION OF A BLAST LOADED CIRCULAR FLAT PLATE

by

GEORGE THOMAS NOLAN, JR.

A thesis submitted to the Graduate Faculty in partial fulfillment of the requirements for the degree

of

MASTER OF SCIENCE

in

Mechanical Engineering

Approved:

Irvin L. Rees (EHB)
Head, Major Department

Dennis O. Blackketter
Chairman, Examining Committee

R. Goering
Graduate Dean

MONTANA STATE UNIVERSITY
Bozeman, Montana

August, 1969

ACKNOWLEDGEMENT

The author is indebted to the National Science Foundation which provided financial aid for this project.

Grateful acknowledgement is also made of the assistance of Dr. Dennis O. Blackketter, director of this research project, who provided invaluable guidance during the preparation of this thesis.

TABLE OF CONTENTS

LIST OF TABLES

LIST OF FIGURES

ABSTRACT

The purpose of this paper is to present an analytical method for calculating the maximum deflection of a simply supported circular flat plate which is subjected to a blast loading. The method is based on the Modified Galerkin Method, and uses a non-linear stress-strain relationship together with non-linear geometry. Equations of equilibrium are reduced to an ordinary differential equation which, when solved, yields an approximation of the maximum plate deflection.

Calculated maximum deflections are compared to experimental test results of permanently deformed plates.

The calculated deflections are approximately 72% of the magnitude of the test results.

CHAPTER I

INTRODUCTION AND STATEMENT OF PROBLEM

This paper studies the response of simply-supported circular plates which are subjected to a blast pressure applied to one side of the plate. Large plate deflections may be obtained if the applied blast pressure is of adequate magnitude and if it is imposed on the plate for a sufficient period of time.

During the deflection of a plate, any element of the plate is subjected to both bending moments, and membrane forces, either of which may be dominant, depending on whether the deflection is small or large. Also, when undergoing large deflections, the plate material may be stressed beyond its yield point into the non-linear stress-strain region. The complete analysis of the blast loaded plate deflection problem should consider deformations through the regions of both elastic and non-linear strains while also recognizing bending and stretching effects.

Wang (1)* developed a method of calculating the permanent deformation of a simply supported circular plate subjected to a blast loading based on a plastic rigid theory. The method considered bending moments dominant, and did not include membrane forces.

Hoffman (2) used Wang's plastic rigid theory in his thesis to calculate the permanent deflection of simply supported circular aluminum plates subjected to air blasts.

*Numbers within parenthesis refer to references.

As part of his thesis, Hoffman also did experimental work and fired explosive charges on several test plates, then compared the actual deformation with the theoretical results. He found that Wang's theory greatly overestimates the plate deflection, especially for small plate thicknesses.

May (3), in his thesis presented to Montana State University, developed an analytical method incorporating a non-linear stress-strain relationship to predict deflections of circular plates subjected to blast loads. The analysis considered bending effects, but did not consider stretching of the middle plane of the plate. May's analysis also overestimated the plate deflection, and he suggested that both bending and stretching effects be considered.

Jones (4) extended Wang's work and considered both bending moments and membrane forces in his analysis of a simply supported circular plate. The analysis considered small deflections, and used a plastic rigid theory.

The purpose of this paper is to present the development of an analytical method for calculating the deflection of a simply supported circular flat plate subjected to a blast type loading. The method recognizes large deflections and uses equilibrium equations together with a non-linear stress-strain relationship while considering both bending and stretching effects. The Modified Galerkin Method was used to reduce the governing partial differential equations of equilibrium to a non-linear ordinary differential equation in time. A solution to the ordinary differential equation expressed the deflection as a function of time. The time derivative of the deflection solution was used to express the plate velocity as a function of time. By solving the deflection and velocity equations simultaneously, the maximum plate deflection could be calculated.

This method determines only the maximum deflection of a blast loaded circular flat plate. A method of predicting the permanent deformation resulting from a given maximum deflection has not been developed.

CHAPTER II

THEORETICAL ANALYSIS

2.1 Equilibrium Equations

A cylindrical coordinate system (r, Θ, z) with its origin at the center of the undeformed middle surface of the plate was chosen with the positive z axis directed downward (Fig. 1).

D'Alembert's principle was used to express the dynamic problem as a static problem. The principle states that a mechanical system in motion is always in a state of dynamic equilibrium under all the forces, including the inertia forces, which act on the system (5).

An element of unit thickness from the deformed plate in an equilibrium position is shown in Fig. 2 with all the forces acting on it including an inertia force and an applied pressure. The forces and moments shown are force per unit length, and moment per unit length, respectively. Subscripts r and t signify the radial and tangential directions.

Loading is assumed to be symmetric about the center of the plate; therefore, shear forces are not developed on the tangential face.

A summation of forces in the z direction was expressed as follows:

$$N_r r d\Theta \sin(-\beta) - (N_r + \frac{\partial N_r}{\partial r} dr)(r + dr)d\Theta \sin(-\beta + d\beta)$$

$$-Q_r r d\Theta \cos(-\beta) + (Q_r + \frac{\partial Q_r}{\partial r} dr)(r + dr)d\Theta \cos(-\beta + d\beta)$$

$$-\rho r dr d\Theta \ddot{w} + P r dr d\Theta = 0 \qquad (1)$$

Equation (1) was then simplified by neglecting higher than second order terms and re-written in the following

form:

$$\Sigma F_z = \{-N_r \sin(-\beta) - \frac{\partial N_r}{\partial r} r \sin(-\beta) + Q_r \cos(-\beta) + \frac{\partial Q_r}{\partial r} r \cos(-\beta) - \rho \ddot{w} r + Pr\} dr d\theta \quad (2)$$

Where, ρ is the mass of the plate per unit area.

$\ddot{w}$ is the acceleration of the plate in the z direction.

β is the angle that the radial centerline of the element makes with the radial axis.

Nr is the normal force per unit length on the radial face of the element.

Q_r is the shear force per unit length on the radial face.

P is the applied blast pressure.

To simplify the summation, angle $-\beta + d\beta$ was considered equal to angle $-\beta$.

A summation of forces in the radial direction which, for simplicity, neglected the horizontal components of the pressure and inertia forces gave:

$$-N_r \, r d\theta \cos(-\beta) + (N_r + \frac{\partial N_r}{\partial r} dr)(r + dr) d\theta \cos(-\beta + d\beta)$$

$$-Q_r r d\theta \sin(-\beta) + (Q_r + \frac{\partial Q_r}{\partial r} dr)(r + dr) d\theta \sin(-\beta + d\beta)$$

$$-2N_t \frac{d\theta}{2} dr = 0 \quad (3)$$

Equation (3) was also simplified by neglecting higher than second order terms and was re-written as:

$$\Sigma F_r = \{N_r \cos(-\beta) + r \frac{\partial N_r}{\partial r} \cos(-\beta) + Q_r \sin(-\beta) + r \frac{\partial Q_r}{\partial r} \sin(-\beta) - N_t\} dr d\theta \quad (4)$$

Where N_t is the normal force per unit length acting on

the tangential face.

A summation of moments about the right-hand radial face of the element was expressed as follows:

$$M_r r d\Theta - N_r r d\Theta dr \sin(-\beta) + N_r r d\Theta dw \cos(-\beta)$$

$$+ Q_r r d\Theta dr \cos(-\beta) + Q_r r d\Theta dw \sin(-\beta)$$

$$-(M_r + \frac{\partial M_r}{\partial r} dr)(r + dr) d\Theta + 2N_t \frac{d\Theta}{2} dr \frac{dw}{2} + 2M_t \frac{d\Theta}{2} dr$$

$$-P r dr d\Theta \frac{dr}{2} + \rho \ddot{w} r dr d\Theta \frac{dr}{2} = 0 \qquad (5)$$

Equation (5) was then simplified by discarding the higher order terms, and rearranged to express the shear force Q_r in terms of the bending moments as:

$$Q_r = \frac{\partial M_r}{\partial r} \cos(-\beta) + \frac{1}{r} M_r \cos(-\beta) - \frac{1}{r} M_t \cos(-\beta) \qquad (6)$$

Where M_r and M_t are the moments per unit length acting on the radial and tangential faces, respectively. Q_r could then be eliminated from equations (2) and (4) by expressing it in terms of the moments.

The radial and tangential forces per unit length were then expressed in terms of the radial and tangential stresses as follows:

$$N_r = \int_{-\frac{h}{2}}^{\frac{h}{2}} \sigma_r dz^* \qquad (7)$$

$$N_t = \int_{-\frac{h}{2}}^{\frac{h}{2}} \sigma_t dz^* \qquad (8)$$

Where h is the thickness of the plate.

The radial and tangential bending moments per unit length were defined by summing moments about the center-

line of the plate in the following manner;

$$M_r = \int_{-\frac{h}{2}}^{\frac{h}{2}} \sigma_r z^* dz^* \tag{9}$$

$$M_t = \int_{-\frac{h}{2}}^{\frac{h}{2}} \sigma_t z^* dz^* \tag{10}$$

Where z^* is the distance from a radial center-line to the element where the normal or tangential stress is acting. z^* is at all times normal to the plate center-line.

The equilibrium equations (2) and (4) are the governing partial differential equations of the system.

2.2 Stress-Strain Relationship

The radial strain was expressed in terms of the displacement.

In Fig. 3, line A-B of length dr is oriented in an r-z coordinate system. Line A-B is displaced in the plane of the coordinate system to position A'-B' and in the final position has attained the length ds. The displacement components of point A with respect to the r-z coordinate system are u and w, respectively. The elongation of line A-B in the r direction is $\frac{\partial u}{\partial r}$ dr, and the elongation in the z direction is $\frac{\partial w}{\partial r}$ dr. The length of line A'-B' is calculated by the pythagorean theorem as:

$$ds = \sqrt{\left(dr + \frac{\partial u}{\partial r} dr\right)^2 + \left(\frac{\partial w}{\partial r} dr\right)^2}$$

By performing the internal multiplication and then expressing ds with a binomial expansion considering terms no higher than second order, ds may be expressed as:

$$ds = dr\left[1 + \frac{\partial u}{\partial r} + \frac{1}{2}\left(\frac{\partial u}{\partial r}\right)^2 + \frac{1}{2}\left(\frac{\partial w}{\partial r}\right)^2\right]$$

The strain in the radial direction, ε_r, could then be defined in terms of the displacements u and w as:

$$\varepsilon_r = \frac{ds-dr}{dr} = \frac{\partial u}{\partial r} + \frac{1}{2}\left(\frac{\partial u}{\partial r}\right)^2 + \frac{1}{2}\left(\frac{\partial w}{\partial r}\right)^2 \qquad (11)$$

Because of the symmetry of deformed shapes that have resulted from blast induced deflections, the tangential strain was expressed as a function of the radial displacement only. In Fig. 4, line C-D of length $rd\theta$ is oriented in an r-θ coordinate system. Line C-D is displaced in the radial direction an amount u to the position C'-D'. The strain in the tangential direction was then defined in terms of the radial displacement u as:

$$\varepsilon_t = \frac{(r+u)d\theta - rd\theta}{rd\theta} = \frac{u}{r} \qquad (12)$$

The following non-linear stress-strain relationship was used to approximate the actual stress-strain relation of the plate material:

$$\sigma = \frac{1}{b}\tanh a\varepsilon \qquad (13)$$

By selecting the proper constants a and b, the linear slope and overall position of a certain stress-strain curve could be approximated.

Fig. 5 shows a stress-strain curve for 6061-T6 aluminum, the material used in the test plates. Fig. 5 also shows the non-linear stress-strain curve as compared to the actual curve for a one-dimensional stress-strain relationship.

Data for the actual stress-strain curve (6) is a composite of various rates of loading from .07 in./in.-sec. through 2700 in./in.-sec. This indicates that the test material is not strain-rate sensitive at relatively low loading rates. Test data, however, was not available for higher rates of strain.

The following relationships were assumed to express the stresses in terms of the strains for the two-dimensional stress system:

for the radial direction,

$$\nabla r = \frac{1}{b} \tanh \left\{ \frac{a}{1-\upsilon^2} \left[\varepsilon_r + \upsilon \varepsilon_t \right] \right\} \tag{14}$$

and for the tangential direction,

$$\nabla t = \frac{1}{b} \tanh \left\{ \frac{a}{1-\upsilon^2} \left[\varepsilon_t + \upsilon \varepsilon_r \right] \right\} \tag{15}$$

Where a value of $\upsilon = .3$ was assumed for Poisson's ratio.

By incorporating equations (11), (12), (13), (14) and (15) into equations (7) and (8), the radial and tangential forces per unit length could be redefined in terms of the displacements as:

$$N_r = \int_{-\frac{h}{2}}^{\frac{h}{2}} \frac{1}{b} \tanh \left\{ \frac{a}{1-\upsilon^2} \left[\frac{\partial u}{\partial r} + \frac{1}{2} \left(\frac{\partial u}{\partial r} \right)^2 + \frac{1}{2} \left(\frac{\partial w}{\partial r} \right)^2 + \upsilon \frac{u}{r} \right] \right\} dz^* \tag{16}$$

$$N_t = \int_{-\frac{h}{2}}^{\frac{h}{2}} \frac{1}{b} \tanh \left\{ \frac{a}{1-\upsilon^2} \left[\frac{u}{r} + \upsilon \left(\frac{\partial u}{\partial r} + \frac{1}{2} \left(\frac{\partial u}{\partial r} \right)^2 + \frac{1}{2} \left(\frac{\partial w}{\partial r} \right)^2 \right) \right] \right\} dz^* \tag{17}$$

Also, equations (9) and (10), the radial and tangential moments per unit length could be redefined in terms of the displacements as:

$$M_r = \int_{-\frac{h}{2}}^{\frac{h}{2}} \frac{z^*}{b} \tanh \left\{ \frac{a}{1-\upsilon^2} \left[\frac{\partial u}{\partial r} + \frac{1}{2} \left(\frac{\partial u}{\partial r} \right)^2 + \frac{1}{2} \left(\frac{\partial w}{\partial r} \right)^2 + \upsilon \frac{u}{r} \right] \right\} dz^* \tag{18}$$

$$M_t = \int_{-\frac{h}{2}}^{\frac{h}{2}} \frac{z^*}{b} \tanh \left\{ \frac{a}{1-\upsilon^2} \left[\frac{u}{r} + \upsilon \left(\frac{\partial u}{\partial r} + \frac{1}{2} \left(\frac{\partial u}{\partial r} \right)^2 + \frac{1}{2} \left(\frac{\partial w}{\partial r} \right)^2 \right) \right] \right\} dz^* \tag{19}$$

Thus the governing equations (2) and (4) can be expressed in terms of the displacements u and w.

The analysis up to this point may be summarized as follows:

The equilibrium equations (2) and (4) were developed to form the governing partial differential equations of the system and are in terms of the forces acting on the plate element.

All internal plate forces and moments were then expressed in terms of radial and tangential stresses.

Relationships were developed to define the strains in terms of radial and transverse displacements u and w.

A non-linear stress-strain relationship was then used together with strain-displacement relationships to express the internal plate forces in terms of the displacements u and w.

By substituting equations (6) and (16) through (19), into the governing partial differential equations (2), and (4), all terms except the pressure and inertia terms could be expressed in terms of the displacements u and w.

2.3 Loading Function

The applied blast pressure loading P was represented by the following decaying exponential function:

$$P = pe^{-kt} \tag{20}$$

Fig. 6 shows the pressure-time relationship of an actual bomb blast compared to the exponential function.

As part of his research, Hoffman (2) experimentally determined the peak pressure p and the impulse I, for each of a series of blast loadings on plates of various thicknesses. The impulse I is defined as the positive area under the pressure-time curve of an actual bomb blast. For this analysis, Hoffman's impulse data was redefined in terms of a decaying exponential function as:

$$I = \int_0^\infty P dt = \int_0^\infty p e^{-kt}\, dt = \frac{p}{k} \qquad (21)$$

Hoffman's pressure and impulse data could then be used to define the constant K in equation (21) as:

$$K = \frac{p}{I} \qquad (22)$$

2.4 Governing Differential Equations

The elemental equilibrium equations (2) and (4) form the governing differential equations of the system. A simultaneous solution of these equations would describe the plate deflection. In abreviated form, equations (2) and (4) become, for the horizontal or radial direction:

$$\sum F_r = 0 \qquad (23)$$

and for the vertical or transverse direction:

$$\sum F_z = 0 \qquad (24)$$

Equation (24), if rewritten to separate pressure and inertia terms becomes:

$$-\ddot{w}\rho r + \sum \tilde{F}_z = -Pr \qquad (25)$$

where the $\tilde{F}_z$ summation signifies that the pressure and inertia terms have been separated from the total F_z summation.

The governing partial differential equations as expressed above are not readily solvable by conventional techniques.

2.5 Modified Galerkin Method

The Modified Galerkin Method was used to reduce the governing partial differential equations to an ordinary non-linear differential equation in time which when solved would permit the plate displacement to be determined.

The Modified Galerkin Method is one version of the method of weighted residuals. This method uses assumed solutions to the governing equations which satisfy the displacement boundary conditions, but not necessarily the force boundary conditions. Assumed solutions to the governing differential equations probably will not satisfy the equations at every location in the plate; therefore, errors, or residuals will result. Since the terms of the governing equations represent a summation of forces, the residuals will be the errors in those forces. If the force residuals are then given virtual displacements considered to be weighting functions, in the assumed displacement modes, the force times displacement products may be considered to have the units of work. The Modified Galerkin Method may be interpreted as requiring that the virtual work done by all forces during a virtual displacement in each of the assumed modes from an assumed displacement shape be identically zero. The modified method is different from Galerkin's conventional method in that the assumed displacement mode shapes, or rather the assumed solutions to the differential equations do not have to satisfy the force boundary conditions. Only the displacement boundary conditions must be satisfied. If the assumed solution does not satisfy the force boundary conditions, then the virtual work done by forces at the boundary, or plate edge, during the virtual displacement must be added to the virtual work done by the internal forces.

Test results (2) have indicated that a simply supported circular plate which has been permanently deformed by a blast loading acquires a dished shape symmetric about the plate center. The test results also

showed that for any large transverse deflection, there is an accompanying radial deflection directed inward towards the center of the plate. This implies that the governing partial differential equations (24) and (25) are each functions of both the radial and the transverse displacements u and w.

Equations were selected to act as a set of assumed solutions to the set of governing partial differential equations. The assumed solutions for the transverse and radial displacements are:

$$w = q_2 \cos \alpha r \tag{26}$$

$$u = q_1 \left(1 - Z_f Z^*\right) \sin \alpha r \tag{27}$$

Where $\alpha = \frac{\pi}{2R}$, and where R is the radius of the simple support circle.

These assumed solutions approximate the deformed plate shape and also satisfy the displacement boundary conditions. For the transverse deflection w, equation (26) permits maximum deflection to be obtained at the plate center (r = 0), and satisfies the displacement boundary conditions by allowing no deflection to occur at the radius of the simple support (r = R). It also describes deflections as being symmetric about the radial center of the plate. From equation (26), the virtual displacement or weighting function for the vertical mode, Φ_2, was defined as:

$$\Phi_2 = \frac{\delta w}{\delta q_2} = \cos \alpha r \tag{28}$$

Internal bending moments were declared identically zero in the development of an expression for the shear force Q_r. However, bending moments might be calculated at the plate edge if the assumed solution did not satisfy the edge boundary condition. To account for this error,

the virtual work was also calculated at the plate edge for a virtual rotation. The virtual displacement in the rotational mode was defined as:

$$\Phi_m = \frac{\delta\left(\frac{\partial w}{\partial r}\right)}{\delta q_2} = -\alpha \sin \alpha r \qquad (29)$$

The angle β that the radial center line of the deformed plate makes with the radial axis, as shown in Fig. 2, could then be described from the assumed solution as:

$$-\beta = \tan^{-1}\left(-\frac{\partial w}{\partial r}\right) = \tan^{-1}\left(q_2 \alpha \sin \alpha r\right) \qquad (30)$$

The sine and cosine of angle β were then defined in terms of the assumed solution (26) as:

$$\sin(-\beta) = \frac{-\partial w}{\sqrt{\partial r^2 + \partial w^2}} = \frac{q_2 \alpha \sin \alpha r}{\sqrt{1 + q_2^2 \alpha^2 \sin^2 \alpha r}} \qquad (31)$$

$$\cos(-\beta) = \frac{\partial r}{\sqrt{\partial r^2 + \partial w^2}} = \frac{1}{\sqrt{1 + q_2^2 \alpha^2 \sin^2 \alpha r}} \qquad (32)$$

The assumed solution (26) was also used to define the acceleration for the inertial force term in equation (25) as:

$$\ddot{w} = \frac{\partial^2 w}{\partial t^2} = \ddot{q}_2 \cos \alpha r \qquad (33)$$

In the assumed solution to the radial displacement, equation (27), the sine function permits no radial displacement to occur at the plate center, and describes a maximum radial displacement at the support radius. A value of Z_f equal to minus one-fourth was selected to account for the additional radial displacement, during bending, of any plate element located above or below the radial center-line of the plate. The magnitude of Z_f was selected to represent an average plate deflection of about two inches. It should be noted that the

varying of Z_f by several orders of magnitude had no noticeable effect on the end result of the deflection calculation.

From equation (27), the virtual displacement in the radial mode, $\overset{I}{\phi}_1$, was defined as:

$$\overset{I}{\phi}_1 = \frac{\delta u}{\delta q_1} = (1 - Z_f Z^*)\sin \alpha r \tag{34}$$

The radial and tangential force and moment expressions, equations (16) through (19), had previously been defined in terms of the displacements u and w. The assumed solutions for u and w, equations (26) and (27), were then used to express the displacement components of the force and moment equations as:

$$\frac{\partial w}{\partial r} = -q_2 \alpha \sin \alpha r \tag{35}$$

$$\frac{1}{2}\left(\frac{\partial w}{\partial r}\right)^2 = \frac{1}{2} q_2^2 \alpha^2 \sin^2 \alpha r \tag{36}$$

$$\frac{\partial u}{\partial r} = q_1 \alpha (1 - Z_f Z^*)\cos \alpha r \tag{37}$$

$$\frac{1}{2}\left(\frac{\partial u}{\partial r}\right)^2 = \frac{1}{2} q_1^2 \alpha^2 (1 - 2Z_f Z^* + Z_f^2 Z^{*2})\cos \alpha r \tag{38}$$

It was then obvious that all force and moment expressions were functions of both the radial and tangential displacements q_1 and q_2. The governing differential equations were coupled by the two displacement modes.

The virtual work for the radial or first displacement mode, δW_1, was defined in terms of equations (23) and (34) as:

$$\delta W_1 = \int_{vol} \sum F_r \overset{I}{\phi}_1 dvol + \int_{edge} \sum \left(F_{r\ exter.} - F_{r\ inter.}\Big|_{edge}\right) \overset{I}{\phi}_1 d\ edge \tag{39}$$

This expression also considered the force boundary conditions not satisfied by the assumed solution in conformance with the Modified Galerkin Method.

The external radial forces, $F_{r\ external}$, at the plate edge were known to be identically zero. However, any error in the assumed solution would cause a non-zero internal radial force, $F_{r\ internal}$, to be calculated at the plate edge.

In a similar manner, the virtual work for the second displacement mode, δW_2, was expressed using equations (25), (28) and (29) as;

$$\delta W_2 = -\int_{vol} \ddot{w}\rho r \underline{\Phi}_2 dvol + \int_{vol} \sum \tilde{F}_z \underline{\Phi}_2 dvol + \int_{edge} \sum (F_{z\ external} - F_{z\ internal}\Big|_{edge}) \underline{\Phi}_2 \cdot dedge + \int_{edge} \sum (M_{external} - M_{internal}\Big|_{edge}) \underline{\Phi}_m \cdot dedge = -\int_{area} Pr \underline{\Phi}_2 \cdot darea \qquad (40)$$

This expression again considers any error in the assumed solution by evaluating the virtual work done at the edge of the plate by the edge moments and forces. External moments and forces are identically zero; however, internal moments and forces could be calculated at the plate edge because of the inaccuracy of the assumed solution.

CHAPTER III

PLATE DEFLECTION

3.1 Integration of Governing Differential Equations

The governing equations of the system are each functions of both q_1 and q_2. Since the purpose of this analysis was to determine only the transverse deflection of the plate q_2, it was necessary that the second mode virtual work expression, equation (40), be reduced to a function of q_2 alone. This was accomplished by numerically integrating the first mode virtual work expression, equation (39), through a range of arbitrarily selected radial and transverse displacements. Because of the complexity of the equations, numerical integration was performed with the aid of a digital computer. The relationship between the two assumed displacement modes was obtained by noting which arbitrarily assigned numerical values of q_1 and q_2 would cause the calculated virtual work δW_1 to be identically zero. Fig. 7 shows the line of zero virtual work calculated through the assumed radial and transverse displacement ranges for plate thickness of 1/8, 1/4 and 3/8 inches. From the curve of Fig. 7, q_1 could be expressed as a polynomial function of q_2 of the form

$$q_1 = -.000464q_2^5 + .00349q_2^4 - .00605q_2^3 - .0219q_2^2 + .00872q_2 \tag{41}$$

This relationship was valid for the three plate thicknesses considered by this analysis.

With the radial displacement q_1 then defined as a function of the transverse displacement q_2, the second mode virtual work expression, equation (40), could be expressed as a function of q_2 only.

The virtual work in the second displacement mode, δW_2, was then calculated, using the digital computer and numerical techniques, over a range of transvere displacements for several different plate thicknesses. The results are illustrated in Fig. 8.

The virtual work as a function of the assumed displacement was considered comparable to a non-linear force vs. deflection relationship of a spring, as would be part of a vibrations-type problem.

3.2 Governing Differential Equation

The system was then ready to be expressed as a non-homogenous second-order ordinary differential equation having one degree of freedom, and resembling the forced vibrations-type problem. The equation of motion was of the form:

$$A\ddot{q}_2 + B_{(q_2)}q_2 = Cpe^{-kt} \qquad (42)$$

The $B_{(q_2)}$ prefix to the displacement term q_2 is the slope of some finite section of the second mode virtual work vs. q_2 curve, which will be covered later in this paper.

A and C, the prefixes to the acceleration and pressure terms respectively, were calculated by integrating the elemental forces with their virtual displacements over the region of the plate as follows:

$$\delta W_2 \text{ pressure} = \int_0^{2\pi}\int_0^{r} Pr\,\phi_2 dr d\theta, \text{ where } P = pe^{-kt}$$

$$= 2\pi\left(\frac{r\alpha - 1}{\alpha 2}\right)pe^{-kt}$$

$$= Cpe^{-kt} \qquad (43)$$

$$\delta W_{2\ \text{inertia}} = \int_0^{2\pi}\int_0^{r+1} \rho r \ddot{q}_2 \cos\alpha r \Phi_2 \, dr d\theta$$

$$= 2\pi\left[\frac{(r+1)^2}{4} + \frac{(r+1)\sin(\alpha(r+1))}{4\alpha r} + \frac{\cos(\alpha(r+1))}{8\alpha^2} - \frac{1}{8\alpha^2}\right]\ddot{q}_2 \qquad (44)$$

$$= A\ddot{q}_2$$

The limits of the integrals were chosen to match the test (2) conditions. Hoffman's test plates were 26 inches in diameter, and were simply supported on a 24 inch diameter support ring. However, the plates were shielded so that no blast pressure could be applied outside of the support ring of radius r, where r = 12 inches. The inertia of that portion of the plate which extended one inch beyond the support circle was to be considered, hence, the integration limit of r plus one inch.

The general solution to the governing differential equation, is of the following form:

$$q_2 = q_2 \text{ complementary} + q_2 \text{ particular} \qquad (45)$$

for which:

$$q_2 \text{ complementary} = D \sin\sqrt{\frac{B(q_2)}{A}}\, t + E \cos\sqrt{\frac{B(q_2)}{A}}\, t \qquad (46)$$

and;

$$q_2 \text{ particular} = \frac{\frac{c}{a}p}{K^2 + \frac{B(q_2)}{A}}\, e^{-kt} \qquad (47)$$

The constants D and E were then evaluated from the following initial conditions:

1. $q_2(o) = 0$; at time zero the plate has no initial displacement.
2. $\dot{q}_2(o) = 0$; at time zero the plate starts from rest.

The complete displacement and velocity solutions for the system were then expressed as q_2 and $\dot{q}_2$, where:

$$q_2 = \frac{K\frac{C}{A}p}{\sqrt{\frac{B(q_2)}{A}}\left(K^2 \quad \frac{B(q_2)}{A}\right)} \sin\sqrt{\frac{B(q_2)}{A}}\, t - \frac{\frac{C}{A}p}{K^2 \quad \frac{B(q_2)}{A}} \cos\sqrt{\frac{B(q_2)}{A}}\, t + \frac{\frac{C}{A}pe^{-kt}}{K^2 \quad \frac{B(q_2)}{A}} \tag{48}$$

$$\dot{q}_2 = \frac{K\frac{C}{A}p}{K^2 \quad \frac{B(q_2)}{A}} \cos\sqrt{\frac{B(q_2)}{A}}\, t + \frac{\sqrt{\frac{B(q_2)}{A}}\,\frac{C}{A}p}{K^2 \quad \frac{B(q_2)}{A}} \sin\sqrt{\frac{B(q_2)}{A}}\, t - \frac{K\frac{C}{A}pe^{-kt}}{K^2 \quad \frac{B(q_2)}{A}} \tag{49}$$

3.3 Solution of the Differential Equation

The maximum deflection of the plate would be attained at the same instant in time that the velocity of the plate had first decayed to zero. A trial and error simultaneous solution to the velocity and displacement equations would be complicated by the non-linear stiffness of the system during its deflection. As a simplification, the stiffness, or rather the virtual work vs. displacement curve as plotted in Fig. 8

was considered to be made up of several linear segments each having a different slope, or stiffness. Fig. 8 was replotted to describe the varying stiffnesses and is shown in Fig. 9. A constant slope or stiffness $B_{(q_2)}$ could then be determined by inspection from each linear segment of the replotted curve. All terms of the displacement and velocity solutions equations (48) and (49) had then been defined.

A series of trial and error solutions, considering the variable stiffnesses, were then made by computer to determine the first non-zero time that the plate velocity reached zero. The maximum plate deflection was then calculated for that elapsed time.

3.4 Results and Discussion

A comparison of the calculated maximum deflection vs. permanent deformations from experimental tests (2) is made in Table I.

TABLE I

DEFLECTION OF SIMPLY SUPPORTED CIRCULAR ALUMINUM (6061-T6) PLATE SUBJECTED TO BLAST LOADING

Thickness (inches)	Pressure (Psi)	Impulse (Psi-Sec)	Text Results Permanent Deformation (inches)	Calculated Maximum Deflection (inches)
.128	185.	.0712	1.238	.89
.128	281.	.0837	1.784	1.12
1/4	582.	.1482	1.519	1.06
1/4	1080.	.1965	2.273	1.57
3/8	620.	.1893	1.218	.87
3/8	2100.	.3600	2.648	1.96

The deflection measured from a permanently deformed plate will always be less than the maximum deflection required to obtain that permanent deformation.

The plate will rebound elastically to the final permanently deformed position.

A calculated maximum deflection will probably be less than an actual maximum deflection if the chosen deflection mode shape is not exactly equal to the true deflection shape. It has been shown that in linear systems, a beam would be deformed to a position which requires a minimum amount of potential energy (7). If the minimum potential energy concept could be extended to apply to the non-linear system, the relative magnitude of the calculated deflections can be explained as follows: by not selecting an exact mode shape for the calculation procedure, the theoretical analysis requires the plate to absorb something more than the minimum amount of energy to deform to the shape of the selected mode. For any given blast pressure and impulse there is only some finite amount of energy available to deform the plate to the shape of the selected mode. The calculated deflections are approximately 72% of the magnitude of the test deflections because of the additional plate stiffness induced by the inaccuracy of the selected mode shape. However, these results are several hundred percent more accurate than those obtained by other calculation procedures (2) and (3).

3.5 Conclusions

The following conclusions were based on the results of this analysis:

1. For large deflections, the primary resistance to deflection is offered by membrane forces.
2. The procedure using the Modified Galerkin Method appears to have merit for analyzing the blast-loaded plate deflection problem.

3.6 Further Studies

Further work should be undertaken to define more accurate deflection mode shapes. For very small transverse deflections in the linear stress-strain region, no radial deflection of the plate center-line will occur. This tends to confirm that the plate stiffness for the small deflections is a function of bending moments alone. Radial displacement, however, will occur within the plate at any finite distance away from the plate center-line. The factor $Z_f Z^*$ as used in this analysis to describe radial deflections of any non center-line point should, therefore, be associated with the transverse deflection q_2 as part of an assumed solution of the form:

$$u = (q_1 - q_2 Z_f Z^*) \sin \alpha r \qquad (50)$$

This form of assumed solution would create no difficulties in the basic calculation procedure.

It is also suggested that a series-type assumed solution be investigated for describing the transverse displacements. A solution of the following form is proposed;

$$w = q_2 (A \cos \alpha r + B \cos 2 \alpha r) \qquad (51)$$

Where; $A + B = 1$

and $A \gg B$

This series form of solution gives a better approximation to the permanently deformed plate shapes obtained by Hoffman (2). Hoffman's test plates were not of a pure sinusoidal shape, but were dished more deeply in the center sections.

The basic deflection calculation might also be extended to handle rectangular plates and consider

different edge support conditions.

A procedure should be developed to predict the permanent deformation and/or rupture that would result from any given maximum deflection.

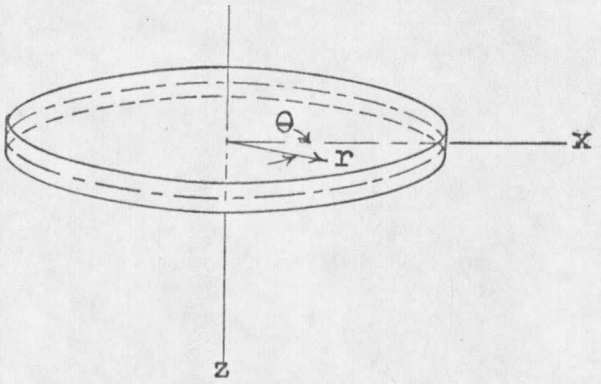

Fig. 1. Cylindrical coordinate system.

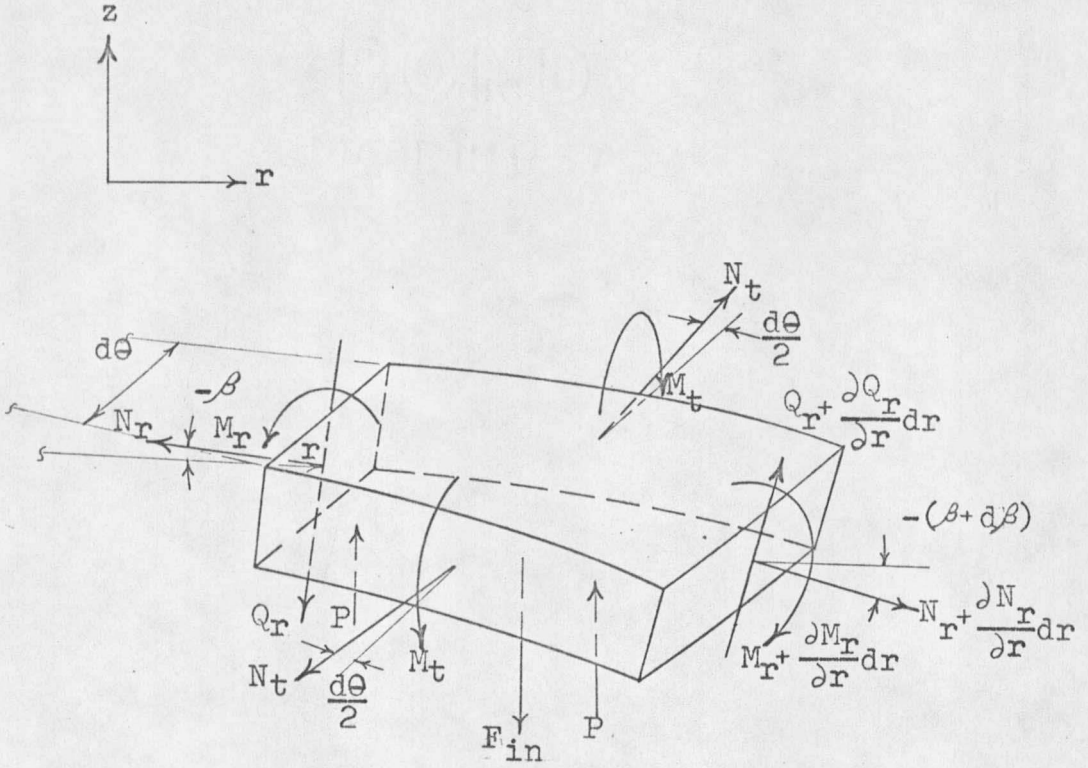

Fig. 2. Free body diagram of plate element.

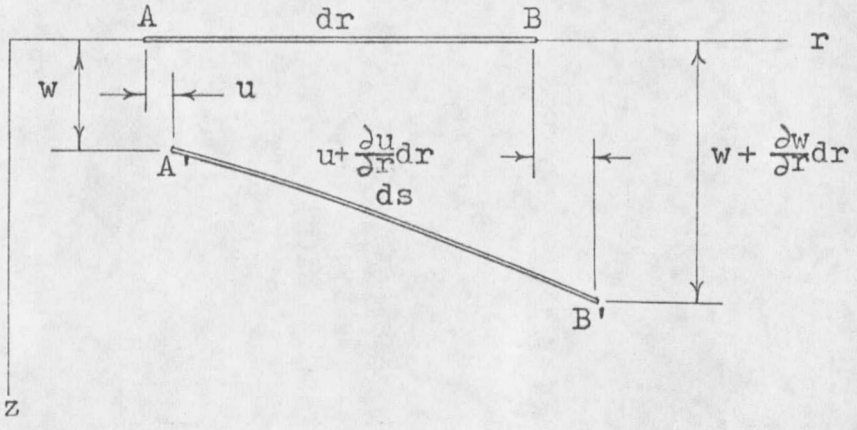

Fig. 3. Displacement of an element in the radial and transverse directions.

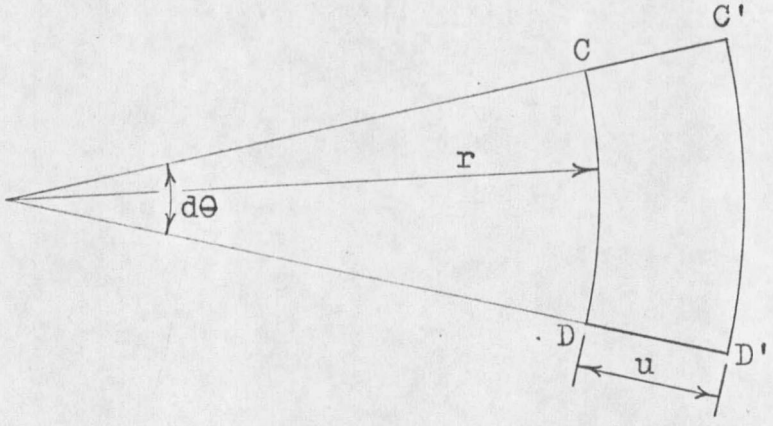

Fig. 4. Displacement of a line in the radial direction.

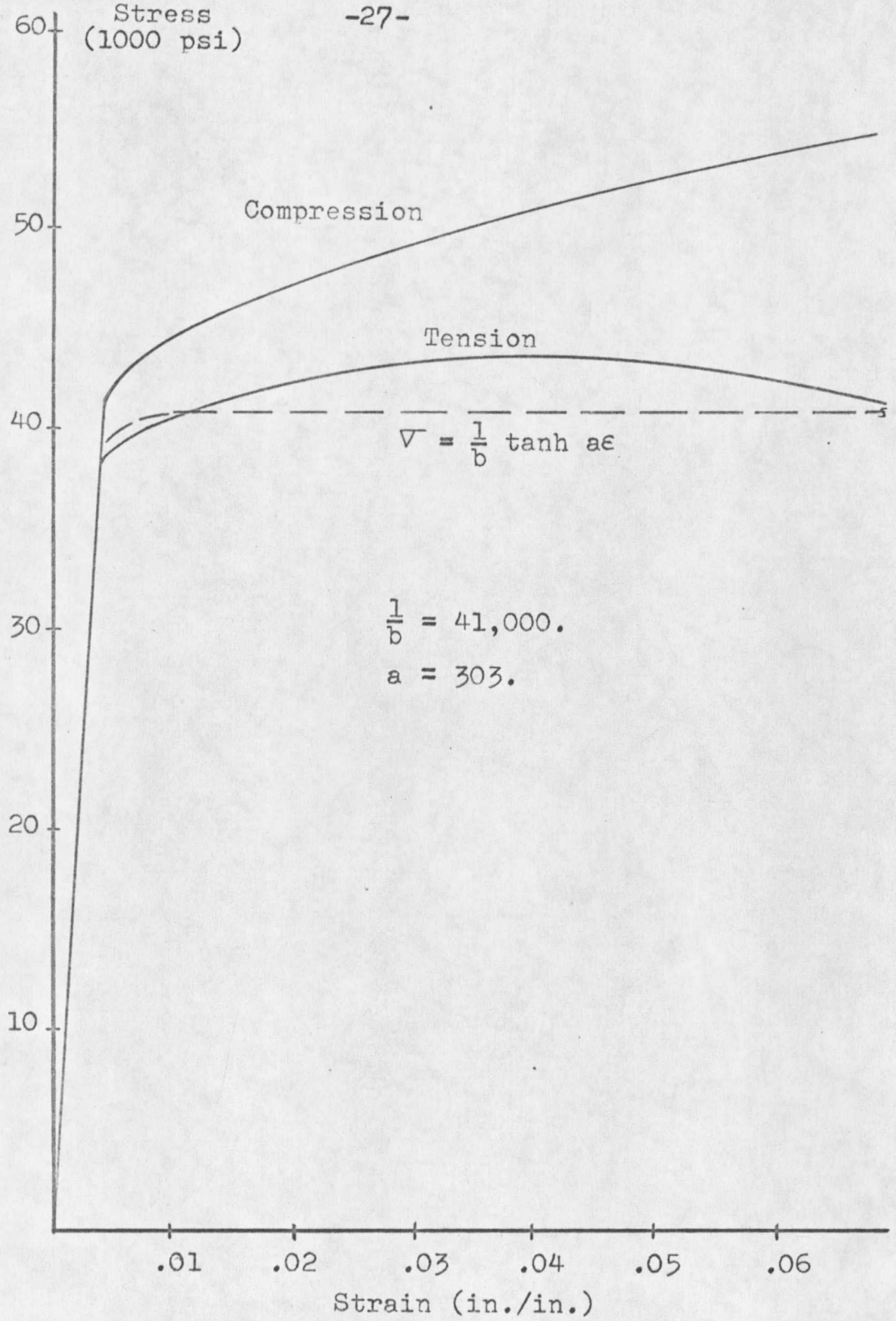

Fig. 5. Actual and non-linear stress-strain curves.

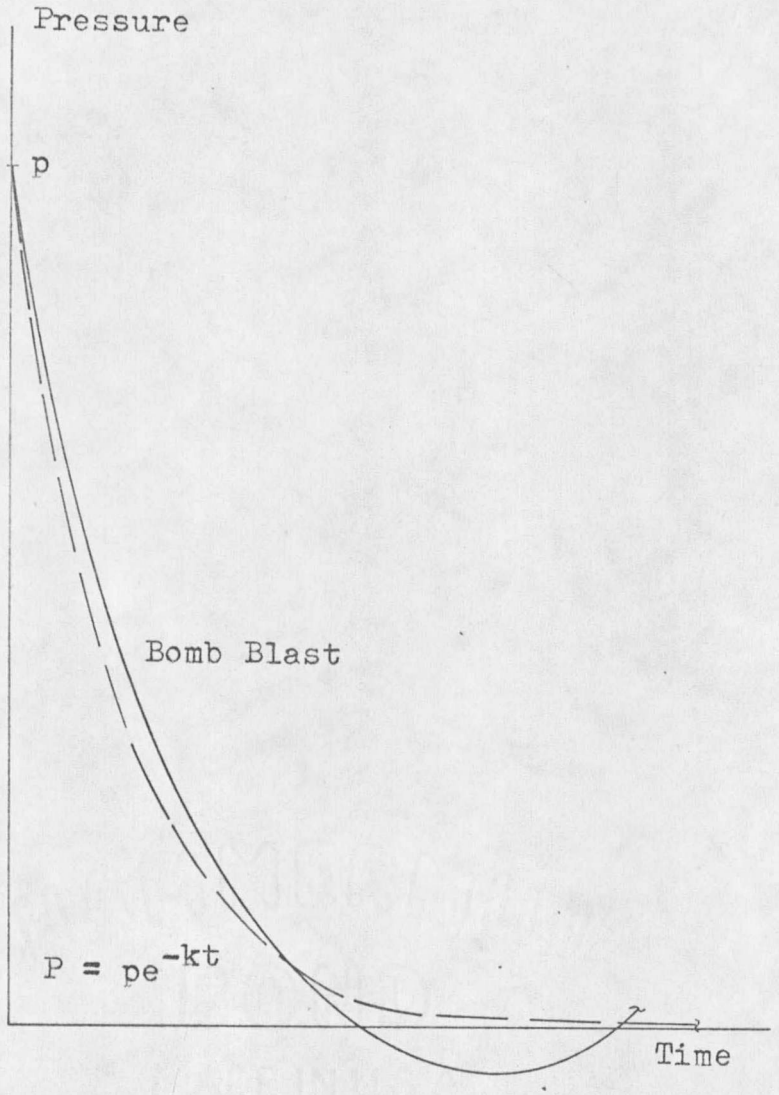

Fig. 6. Pressure-time curve of blast.

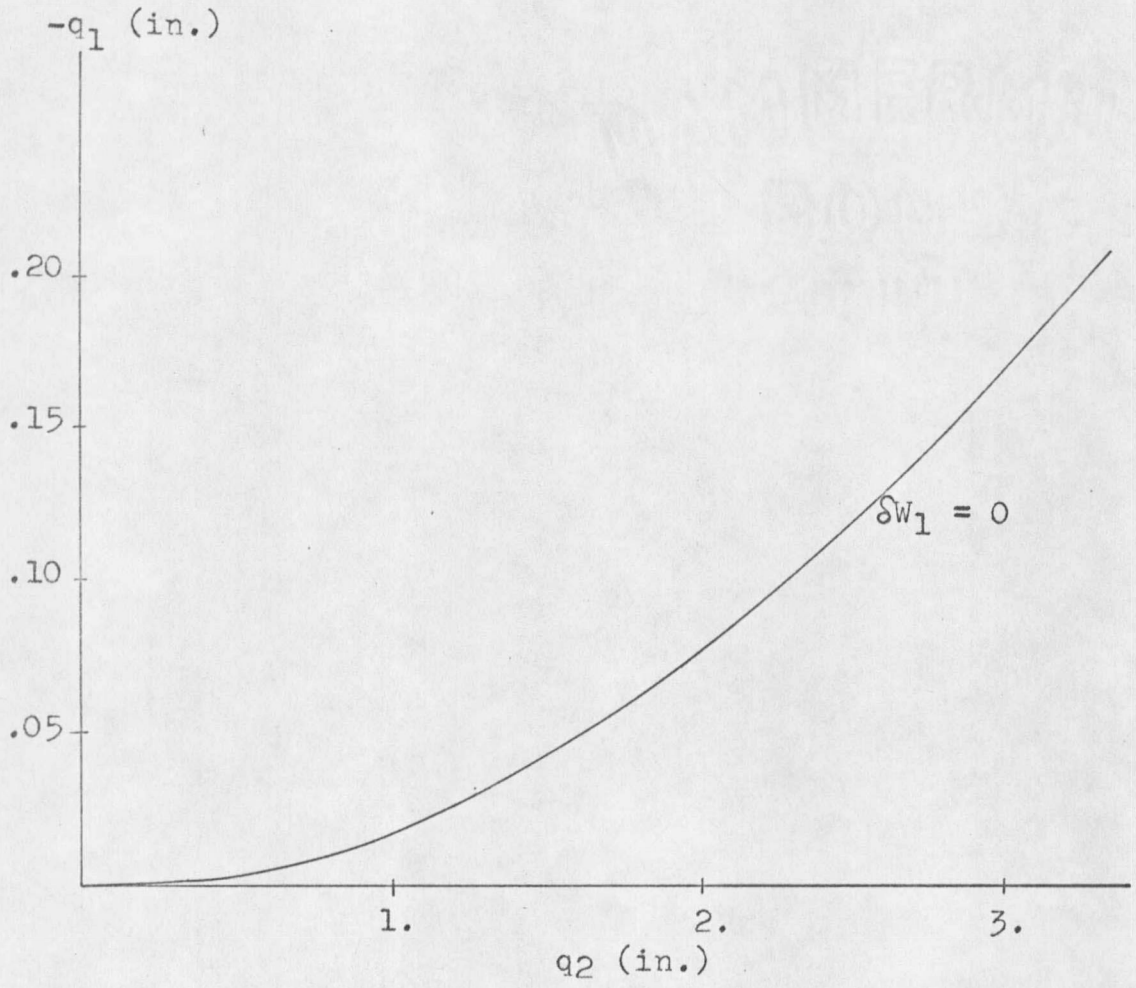

Fig. 7. Displacement mode relationship.

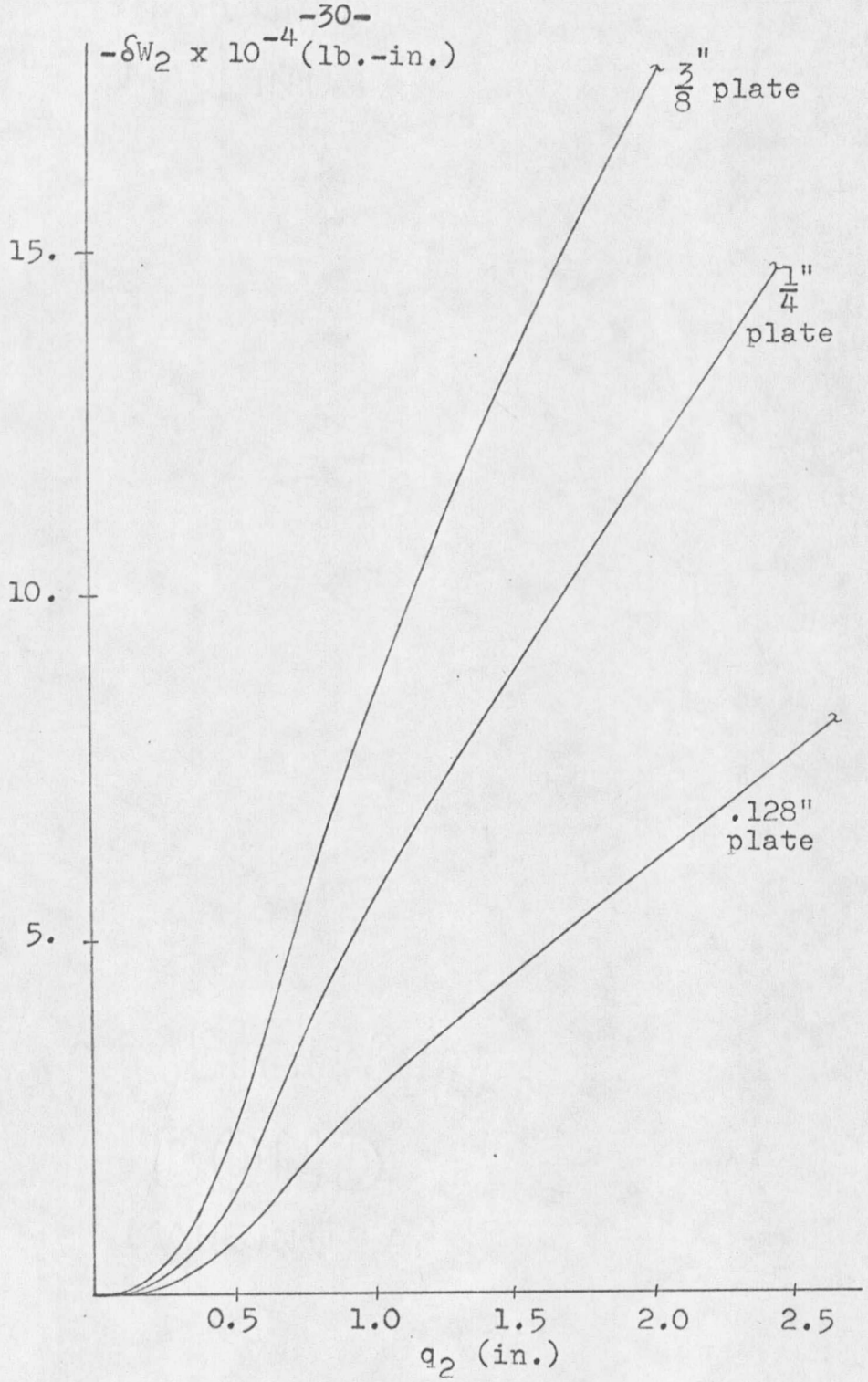

Fig. 8 Calculated virtual work in second displacement mode.

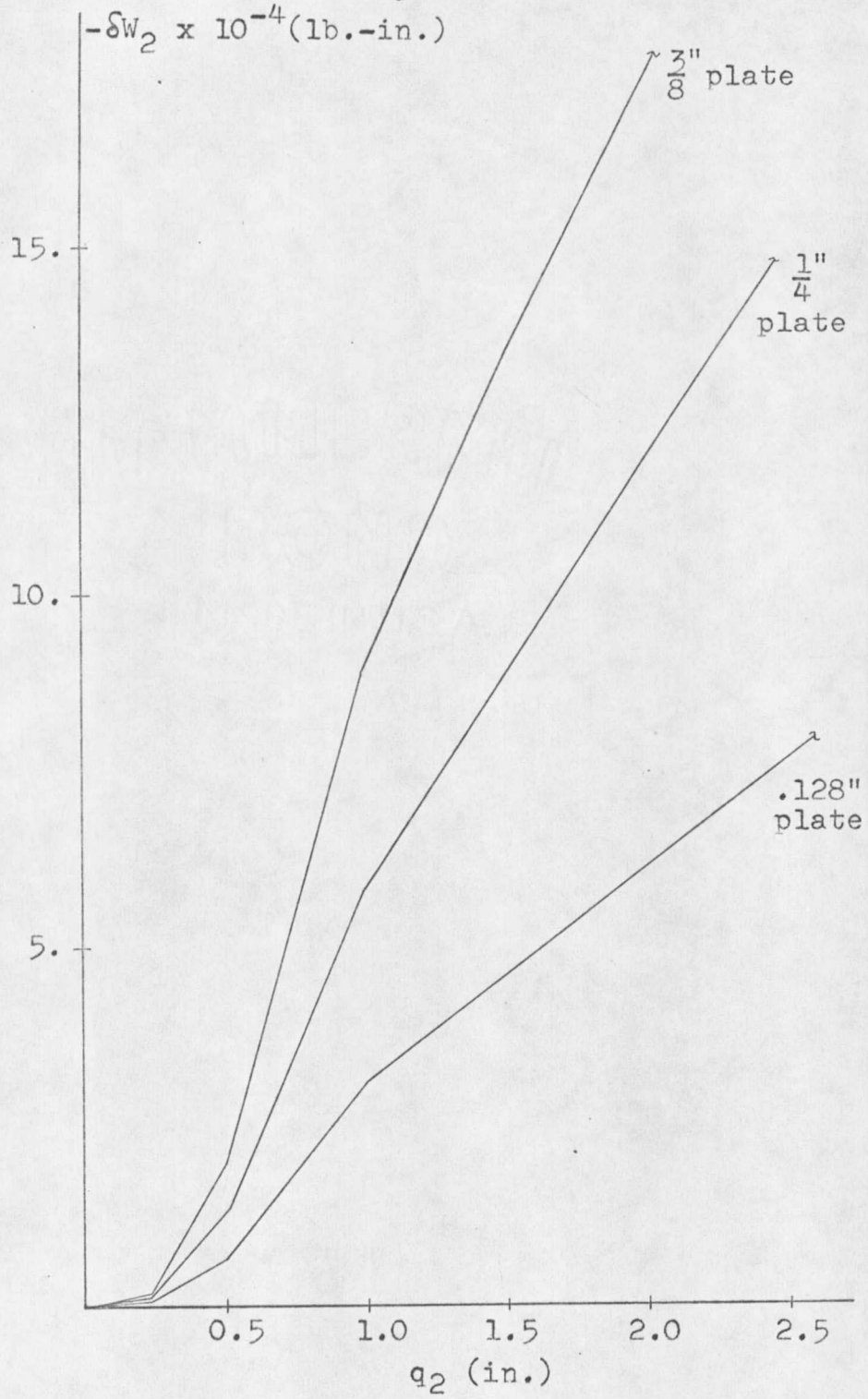

Fig. 9 Modified virtual work curve.

LITERATURE CONSULTED

1. Wang, A. J., "The Permanenet Deflection of a Plastic Plate Under Blast Loading", Technical Report No. 7, Grad. Div. of Applied Math., Brown Univ., Dec., 1953.

2. Hoffman, A. J., "The Plastic Response of Circular Plates to Air Blasts", Master's Thesis, Dept. of Mech. Engrg., Univ. of Delaware, June, 1955.

3. May. L. E., "Deflection of a Circular Plate Subjected to a Blast Loading", Master's Thesis, Dept. of Mech. Engrg., Montana State University, December, 1968.

4. Jones, N., "Impulsive Loading of a Simply Supported Circular Rigid Plastic Plate", Journal of Applied Mechanics, March, 1968.

5. Anderson, R. A., Fundamentals of Vibrations, The Macmillan Company, New York, 1967.

6. "Strain Rate Tests on Aluminum 6061-T6", GM Defense Research Laboratories, General Motors Corporation, TR65-69.

7. Langhaar, H. L., Energy Methods in Applied Mechanics, Wiley, New York, 1962.